COMMUNICATIONS IN SCIENCE AND TECHNOLOGY
Homepage: cst.kipmi.or.id

Material properties extraction of mango (*Mangifera indica*) leaves at ka-band using a waveguide measurement system

Hana Arisesa[a,d], Sevia Mahdaliza Idrus[a,*], Farabi Iqbal[a], M.F.L. Abdullah[b], Yusuf Nur Wijayanto[c], Purwoko Adhi[d]

[a]*Department of Electrical Engineering, Universiti Teknologi Malaysia, Johor Bahru 81310, Malaysia*
[b]*Department of Electrical & Electronic Engineering, Universiti Tun Hussein Onn Malaysia, Johor 86400, Malaysia*
[c]*Research Center for Electronics-BRIN, Jl. Sangkuriang, Bandung 40135, Indonesia*
[d]*Research Center for Telecommunication-BRIN, Jl. Sangkuriang, Bandung 40135, Indonesia*

Article history:
Received: 20 August 2025 / Received in revised form: 25 November 2025 / Accepted: 30 November 2025

Abstract

This study investigates the material properties (permittivity, dissipation factor, and conductivity) of mango leaves (*Mangifera indica*) over the 26–40 GHz Ka-band frequency based on a waveguide measurement system with a vector network analyzer instrument to capture the data. The data analysis employs the Nicolson-Ross-Weir method to extract material properties. The result reveals that the real part of permittivity decreases from about 11.0 to 5.0 with increasing frequency. Meanwhile, the imaginary part of permittivity remains low and stable, suggesting minimal absorption losses. The dissipation factor is consistently below 0.05 along the band. Effective conductivity ranges from 0.2 to 0.6 S/m, with a slight increase at higher frequencies. These findings suggest that at Ka-band frequency, signal degradation through mango foliage is primarily driven by dispersion and scattering rather than strong dielectric absorption. The results provide essential information for improving foliage attenuation models and designing 5G and 6G communication systems in tropical regions. This study provides a reliable Ka-band dielectric dataset for mango leaves that improves the accuracy of tropical foliage-attenuation models and supports more robust 5G/6G link design and deployment in vegetation-dense environments.

Keywords: Permittivity; de-embedding; vegetation; mmWave; mango; fruit

1. Introduction

The advantages of future fifth-generation (5G) and sixth-generation (6G) wireless communication networks include the millimeter-wave (mmWave) spectrum (30–300 Gigahertz [GHz]), which offers the possibility of ultra-reliable high-speed data transmission due to its capacity to accommodate large bandwidths [1-4]. Meanwhile, in terms of market penetration, the majority of 5G technologies still utilize mid-band frequencies (1–6 GHz) for deployment, although high-band frequencies have been implemented; only a small number of countries have done so, such as Japan, the United States of America, Europe, China, South Korea, India, Australia, and parts of Southeast Asia [5]. This indicates that the potential of millimeter waves is still important to explore, especially for their worldwide deployment.

Unfortunately, the use of millimeter wave frequencies brings new challenges that need to be addressed, namely the significant attenuation loss due to the higher frequency used [6,7]. In addition, challenges are also faced when implemented in tropical countries with heterogeneous vegetation characteristics, elevated humidity, and dense tropical forests, which can result in greater signal loss [8, 9]. One of the keys to a deeper understanding of the issue of propagation loss due to vegetation is to know the characteristics of vegetation in interacting with electromagnetic signals, as this phenomenon is closely related to signal attenuation and scattering losses.

In tropical regions, dense vegetation elements such as leaves, stems, bark, and soil litter layers store a lot of water and have a complex structure leading to signal dispersion, absorption, and repeated reflections, which can reduce communication performance and result in unpredictable propagation losses [10]. Furthermore, because of their high moisture content and heterogeneous structure, tropical vegetation dielectric responses are extremely frequency-dependent and susceptible to seasonal or even daily fluctuations [11]. Without understanding the characteristics of vegetation material, modeling and simulation of the mmWave propagation aspect in these situations are unreliable.

Knowing the characteristic properties of natural materials is not only useful for wireless telecommunications applications

* Corresponding author.
Email: sevia@utm.my
https://doi.org/10.21924/cst.10.2.2025.1768

but can also be utilized for applications in other fields. Moreover, natural materials have advantages over man-made materials in terms of environmental friendliness, availability, and safety. Therefore, research on the characterization of natural materials is widely conducted, such as for the material absorbers [12,13], insecticide [14], remote sensing [15,16], and agriculture.

Material characteristics can be described by several main parameters, such as dielectric constant [17], permittivity [18], permeability [19], and conductivity [20]. These parameters are frequency-dependent and vary with factors such as water content, leaf thickness, and structural composition. Relative electrical permittivity denotes a material's capacity, in the context of food, to absorb and retain energy when subjected to an electric field. This characteristic affects wave reflection at boundaries and wave attenuation within the materials. Material permeability is how a material can interact with a magnetic field inside. For natural material without any intervention process, it is effectively non-magnetic throughout the entire frequency band. The relation among these parameters can be urgently needed for any application related to electromagnetic wave interaction with material.

Mango (*Mangifera indica*) is one of the popular tropical vegetations, especially in Southeast Asia, not only as a popular horticultural commodity but also as a critical nutrition source, supplying carotenoids, vitamin C, and dietary fiber that bolster food and nutrition [21]. Because of their important uses, mangoes are extensively studied to reveal their characteristic values, not only physically and morphologically, but also electrically. This is important for the development of new methodologies for characterization, quality evaluation, and monitoring of food processing using non-destructive techniques [22].

Mango canopies exhibit electromagnetic behavior dominated by high tissue water content and ionic conduction, yielding a complex permittivity form $\varepsilon(\omega)=\varepsilon'(\omega)-j\varepsilon''(\omega)$ with $\mu r\approx 1$ for non-magnetic plant matter [23]. Tropical phenological cycles—floral induction during the dry season and growth in the wet season—regulate leaf water status and ion composition, resulting in quantifiable diurnal and seasonal fluctuations in permittivity that influence foliage attenuation, depolarization, and backscatter pertinent to remote sensing and terrestrial connections. At the canopy level, leaf orientation, lamina thickness, vein anisotropy, and fruit clustering contribute to multiple scattering and polarization sensitivity, while cuticle roughness modifies the specular and diffuse components of reflection and transmission [24]. Consequently, rigorous electromagnetic (EM) characterization of mango is essential for propagation models, path loss attenuation, link reliability, and sensor performance in mango-dominated tropical landscapes.

Most existing studies on vegetation dielectric properties extraction have focused on microwave frequencies below 20 GHz, with only a limited number of works extending into the Ka-band and higher millimeter-wave ranges [25-27]. Previous investigations have typically examined temperate-region vegetation or relied on bulk, free-space, or coaxial measurement setups, resulting in a lack of high-accuracy waveguide-based characterization data for tropical leaves at Ka-band frequency.

This lack of Ka-band dielectric data for tropical vegetation represents a significant knowledge gap, especially given the increasing use of millimeter-wave frequencies in 5G and emerging 6G systems. The present study addresses this gap by providing one of the first waveguide-based measurements of complex permittivity, loss factor, and conductivity for tropical mango leaves across the Ka-band, thereby contributing new and relevant insights into vegetation–wave interactions in tropical environments.

This study aims to characterize the dielectric behavior of tropical mango leaves (*Mangifera indica*) using a waveguide-based measurement technique to obtain complex permittivity, relative dielectric constant, loss factor, and conductivity in the Ka-band—an area that has not been extensively explored at millimeter-wave frequencies. Although the dielectric response of biological tissues can be influenced by moisture content, cellular structure, and, to a lesser extent, chemical composition, the dominant mechanism at Ka-band arises from water-related relaxation rather than specific phytochemical constituents. Therefore, the focus of this work is to provide representative dielectric characterization rather than detailed chemical profiling. To minimize sample heterogeneity, leaf specimens were randomly selected from the same species and growth stage, and their moisture content was determined using the gravimetric wet–dry method prior to measurement, ensuring consistency and reducing biological variability. In addition, this research also presents the investigation of leaf sample thickness and its impact on the extracted dielectric parameters, an aspect rarely discussed in existing millimeter-wave vegetation studies.

2. Material and Methods

2.1. Mango leaves sample preparation

In this work, samples from mango leaves were used as samples under test (SUT). The sample was acquired from the local Indonesian mango tree, which has grown for ten years. The fresh mango leaves were collected directly from the trees. The selection of leaves on the tree is based on random sampling with consideration for not choosing damaged surfaces and young leaves. However, the sample is chosen for similar morphological structure, which is shown in Fig. 1. Then the leaves are washed to remove any dirt adhering to them. In this research, samples were required to be in flat sheet condition for the measurements in the waveguide. Therefore, each leaf was treated by a pressing technique using simple heavy book pressing for 1-3 days to flatten the sample.

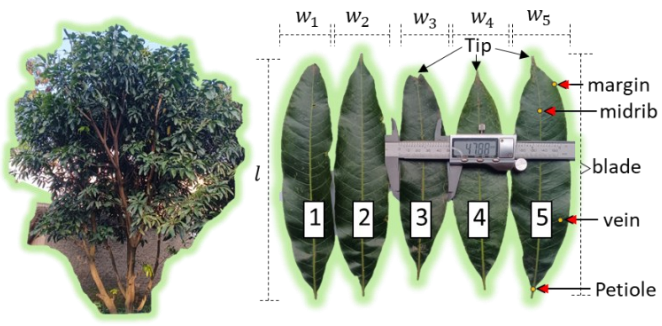

Fig. 1. Sample under test (SUT): mango leaves

The mango leaves were physically characterized in terms of thickness, width, and the length of the leaf. A leaf has a structure consisting of a tip, midrib, margin, vein, blade or lamina, and petiole. For instance, five leaves as depicted in Fig. 1 have been measured. The measurement results for the thickness, width, and length of the leaves are shown in Table 1.

Table 1. Physical characterization of the samples

Leaves	Thickness (mm)	Width (mm)	Length (mm)
1	0.45	56.17	215.81
2	0.42	54.46	222.88
3	0.40	47.88	183.70
4	0.48	53.58	195.25
5	0.41	55.72	213.43

The measurement was carried out using a caliper. The averages of the thickness, width, and length of the samples are 0.432±0.029 mm, 53.564±2.981 mm, and 206.214±14.484 mm, respectively. The most important parameter here is the leaf thickness due to its relation to permittivity material. Note that in a mango tree, the leaves naturally have varying thicknesses between young and old leaves. These thickness differences will naturally affect the calculation of material characteristics.

Moisture content (MC) plays a fundamental role in determining the dielectric behavior of plant tissues, particularly within the microwave and millimeter-wave frequency ranges relevant to this study. In this study, the moisture content of each leaf sample was quantified using the standard gravimetric method, which compares the mass of fresh leaves with their mass after drying to calculate the moisture content of the sample used in the experiment. The moisture content was calculated as the relative difference between the fresh and dry weights, providing an accurate estimation of the water fraction within each sample. This information is essential for interpreting the observed variations in permittivity across different plant materials, as water content strongly influences polarization mechanisms and dielectric dispersion at high frequencies. The standard formula for moisture content is as follows:

$$Moisture\ Content\ (MC) = \frac{W_{fresh} - W_{dry}}{W_{fresh}} \times 100\% \qquad (1)$$

(a) (b)

Fig. 2. Measuring of leaf samples; (a) Fresh leaf, (b) Dry leaf

To determine the moisture content (MC) of the sample used as the test specimen (sampel under test—SUT), the MC was calculated using Eq. (1).

This procedure employs an average approach based on randomly selected mango leaf samples consisting of five fresh mango leaves and five oven-dried mango leaves. All samples were weighed using an OPTIMA SCALE OPD-E digital balance, and the measurements were then averaged. The mean weights of the fresh and dried mango leaf samples were subsequently used to compute the MC of the sample employed in the experiment. Fig. 2 depicted the measurement setup for each sample, and Table 2 presents the measured weights of each leaf sample.

Table 2. The measured weights result of each leaf samples

Leaves	Fresh Leaves (g)*	Dry Leaves (g)
1	2.1583	1.0729
2	2.2038	0.7819
3	2.2905	0.7494
4	1.9780	1.3072
5	2.3630	1.2470

* Note: The different fresh leaves used in the measurement

The calculated average fresh leaves is 2.1987±0.0655 (g), and the calculated average dry leaves is 1.0317±0.1154 (g). Using Eq. (1), the moisture content of the SUT is 53.06%±5.44%.

2.2. *Measurement methods and procedures*

A Vector Network Analyzer—VNA (Anritsu MS46322A) has been used to measure the SUT S-parameter (S11, S12, S21, and S22) using the Ka-Band rectangular waveguide, size 28 (WR-28), based on two-port network measurement. Two pairs of coax-to-waveguide adapters, WR-28 Ka Band (26.5─40 GHz) from UIY Inc., are used for guided signal transmission. A calibration based on a coaxial Thru–Reflect–Line (TRL) calibration kit (open, load, through) was performed for the entire frequency band before the measurement was performed. Due to the limited resources, the calibration was only performed for the coaxial input port 1 and output port 2 of the VNA. Meanwhile in the measurement, the fixture (waveguide adaptor and sample holder) was used. This variables will influence the scattering parameter (S-parameter) result that needs to be further compensated in data analysis to eliminate the contribution from the fixture. Fig. 3 shows the setup measurement in this work.

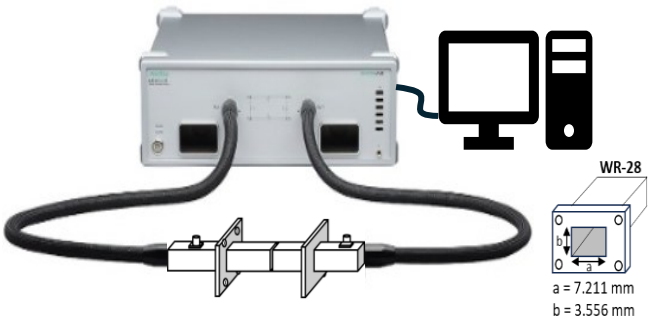

Fig. 3. Setup measurement for this study.

In a waveguide-based VNA measurement system, after calibration is performed on port 1 and port 2 of the VNA over a frequency bandwidth of 26-40 GHz, two fixtures are then connected to each VNA port. The mango leaf samples were cut

to the dimensions of the WR-28 waveguide, 7.112 mm x 3.556 mm, and then placed tightly between two fixtures. The selection of mango leaf samples for this cutting process has no special requirement, just choosing leaves in good condition. In this setup, the dominant mode is TE_{10} with a cutoff frequency of 21.077 GHz. After completing the preparation setup, S-parameter data from the sample under test is recorded for analysis to extract material characteristics.

2.3. *Data extraction analysis*

Material characteristics extraction is a process to determine several material parameters, such as complex permittivity, dielectric constant, dielectric loss, and conductivity of the SUT from the measured S-parameters data. For this purpose, the Nicolson-Ross-Weir (NRW) Method was used. The NRW method is one of the popular ways to extract the permittivity and permeability of a material. The NRW method is suitable for the waveguide-based measurement system using VNA, such as in this study.

The NRW method analyzes the measured S-parameter, especially S_{11} (reflection coefficient at port 1) and S_{21} (transmission coefficient at port 2) from the SUT, to determine a material's complex permittivity (ε), permeability (μ), and conductivity (σ) through a two-port network system. The process of extracting the complex permittivity (ε) from measured S-parameters involves several detailed steps to ensure accurate characterization of the SUT, especially in waveguide measurement systems. First, the measured S-parameters (S_{11} and S_{21}) are obtained using a vector network analyzer (VNA), representing the reflection and transmission responses of the system with the sample inserted.

This raw data proceeds to eliminate the influence of the fixtures (waveguide adapter and holders) that are not part of the sample using the de-embedding method. This method isolates the sample's intrinsic response by mathematically subtracting or compensating for the effects of the measurement setup. In this study, a simplified S-parameter correction de-embedding method was applied to compensate for the presence of the empty sample holder (fixture). The corrected reflection and transmission coefficients were computed using:

$$S_{11corr} = \frac{S_{11meas} - S_{11fixture}}{1 - S_{11meas} * S_{11fixture}} \quad (2)$$

$$S_{21corr} = \frac{S_{21meas}}{S_{21fixture}} \quad (3)$$

where S_{11corr}, S_{11meas}, and $S_{11fixture}$ are the corrected reflection coefficient, the measured reflection coefficient of the SUT, and the measured reflection coefficient without the SUT attached, respectively. S_{21corr}, S_{21meas}, and $S_{21fixture}$ are the corrected transmission coefficient, the transmission coefficient of the SUT, and the transmission coefficient without the SUT attached, respectively.

The NWR method to extract material permittivity has several calculation steps [28-31]. The reflection coefficient (Γ) and transmission coefficient (T) should be derived from the measured S-parameter of the SUT through the intermediate variable complex number D as follows:

$$D = \frac{S_{11corr}^2 - S_{21corr}^2 + 1}{2S_{11}corr} \quad (4)$$

Therefore, the reflection coefficient (Γ) and transmission coefficient (T) can be calculated using the formula

$$\Gamma = D \pm \sqrt{D^2 - 1} \quad (5)$$

$$T = \frac{S_{21corr}}{1 - \Gamma} \quad (6)$$

In Eq. (5), the reflection coefficient (Γ) can finally be extracted from measured S-parameter of the SUT as expected. The important factor is to determine the correct root, which satisfies $|\Gamma|<1$ for the chosen root due to the passive behavior of the material and Eq. (6), and the simplicity of the standard NRW method, for which the transmission coefficient (T) can also be derived using [32]

$$T = \frac{S_{11corr} + S_{21corr} - \Gamma}{1 - (S_{11corr} + S_{21corr})\Gamma} \quad (7)$$

Once the reflection coefficient (Γ) and transmission coefficient (T) have been derived, then the complex relative permittivity (ε_r) is calculated using the relation $\varepsilon_r = n / Z$, where n is the complex refractive index (n) of the material and the impedance (Z) which calculated as follows [32,33]:

$$n = \frac{1}{\beta d} cos^{-1}\left(\frac{1}{2T}\right) \quad (8)$$

$$Z = \frac{(1+\Gamma)^2 - T^2}{(1-\Gamma)^2 - T^2} \quad (9)$$

Material conductivity, which is dependent on the frequency, can be calculated from material complex relative permittivity (ε_r) as follows:

$$\sigma_{eff}(\omega) = \omega \varepsilon_0 \varepsilon_r''(\omega) \quad (10)$$

where ε_0 is permittivity of free space (8.854E-12 F/m) and $\varepsilon_r''(\omega)$ is the imaginary part of the extracted complex relative permittivity of the SUT which has been calculated before. In (8) the thickness of the SUT plays important role in the final result of permittivity extraction.

3. Results and Discussion

The measured S-parameter (magnitude) of the SUT from one slab of fresh mango leaves (*Mangifera indica*) with a thickness of 0.432±0.029 mm from the VNA measurement at Ka-band frequency is depicted in Fig. 4–7. In the Ka-band frequency (26–40 GHz), the magnitude scattering parameters (S_{11}, S_{12}, S_{21}, and S_{22}) are plotted versus frequency. From the S-parameter result it can be inferred that a moderately lossy material with smooth and non-resonant behavior has been described. The forward and reverse transmission magnitudes overlap closely where $|S_{21}| \approx |S_{12}|$ with only a small ripple, indicating good reciprocity and no nonlinear effects. Insertion loss remains roughly in the low tens of dB with weak frequency dependence, while the return losses differ slightly.

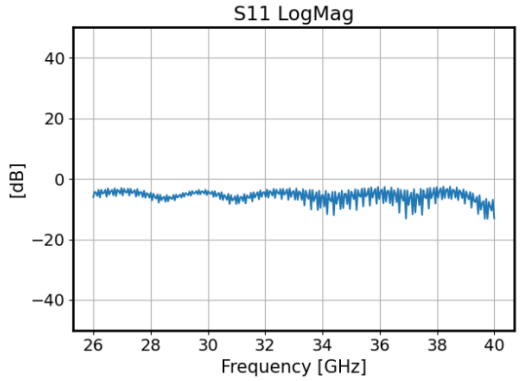

Fig. 4. Measured S-parameter (magnitude of S_{11}) of mango leaves

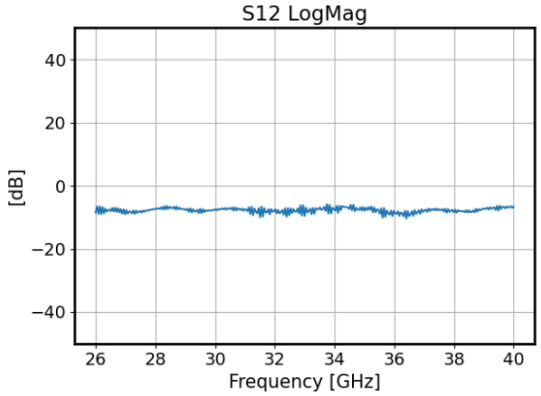

Fig. 5. Measured S-parameter (magnitude of S_{12}) of mango leaves

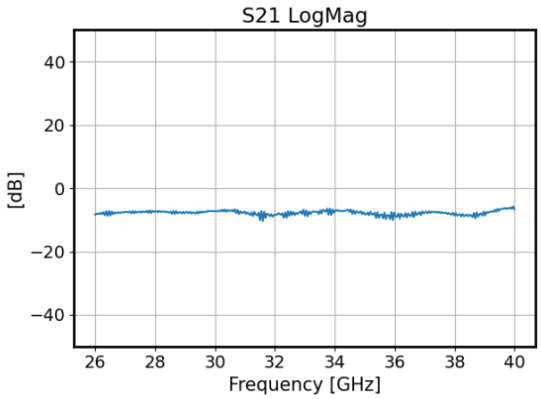

Fig. 6. Measured S-parameter (magnitude of S_{21}) of mango leaves

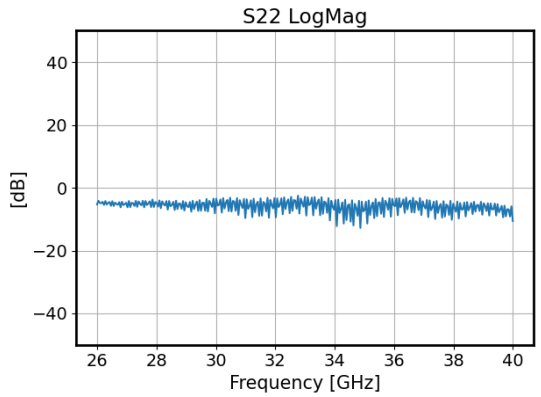

Fig. 7. Measured S-parameter (magnitude of S_{22}) of mango leaves

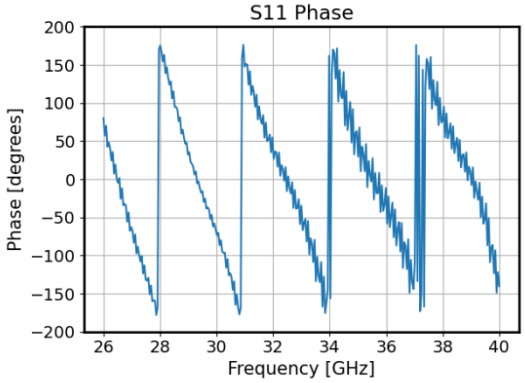

Fig. 8. Measured S-parameter (phase of S_{11}) of mango leaves

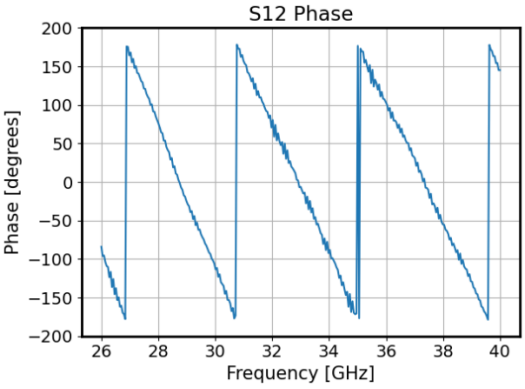

Fig. 9. Measured S-parameter (phase of S_{12}) of mango leaves

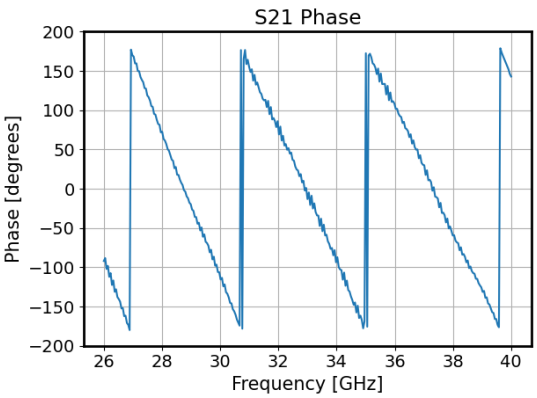

Fig. 10. Measured S-parameter (phase of S_{21}) of mango leaves

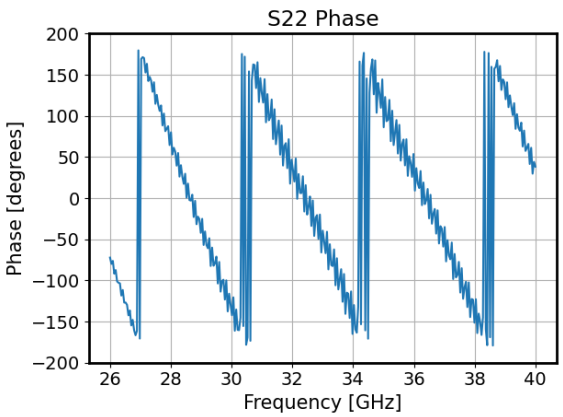

Fig. 11. Measured S-parameter (phase of S_{22}) of mango leaves

In port 1, magnitude of S_{11} is modestly matched (≈−8 to −12 dB) and trends a little worse toward 40 GHz, whereas for port 2, magnitude of S_{22} is generally better matched (≈≤−15 dB). The shallow, quasi-periodic ripple visible on all traces indicates multiple reflections in the fixture or sample stack rather than true resonances. There is no sharp notches or peaks observed. Overall, the data from the mango leaves sample are consistent with a broadband, effectively non-magnetic dielectric element whose response in Ka-band is dominated by attenuation and interface mismatch rather than narrowband resonance.

Fig. 8–11 depicted the S-parameter (phase) of mango leaves. Across the 26–40 GHz Ka-band frequency, the phase scattering parameters S_{11}, S_{12}, S_{21}, and S_{22} are plotted versus frequency. The S-parameter phase responses are dominated by a smooth, nearly linear downward slope with periodicity every ±180°. The transmission phases (S_{21}, S_{12}) track closely, indicating a reciprocal, time-invariant device with no nonlinear effect. The slight superposed ripple is consistent with weak multiple reflections in the fixture. The reflection phases (S_{11}, S_{22}) show similar trends, with stronger ripple at the more poorly matched port, consistent with the log-magnitude S-parameter data.

After obtaining the overall S-parameters (magnitude and phase) from the VNA measurements of the sample material under test, direct extraction of permittivity data is not possible. This relates to the validity of the S-parameter values from the sample under test. The measured S-parameter results are a combination of the S-parameter values from the sample under test and the fixture (waveguide and holder). Considering that the calibration performed in this study was limited only to the coaxial input of the VNA due to lack of a complete calibration instrument. Ideally, the calibration should be done up to the fixture (waveguide and sample holder) so that the S-parameters obtained are purely based on the influence of the sample.

Therefore, de-embedding techniques are needed to eliminate the influence of the fixture. (1) and (2) are used for this purpose. To employ (1) and (2), it is necessary to measure the S-parameters without the sample under test, then denoted as the S-parameter $_{fixture}$.

Fig. 12–15 show the measured magnitude S-parameters in dB without a sample present over the measurement frequency range of 26–40 GHz. It can be concluded that the values of the forward and reverse transmission coefficients (S_{21} and S_{12}) are identical and close to 0 dB across the entire band. This indicates very little transmission loss, demonstrating good matching in the measurement. Conversely, the reflection coefficients (S_{11} and S_{22}) consistently remain below -20 dB, with ripples visible across the entire band. This indicates that the reflection is occurring on the fixture or is caused by its uneven surface.

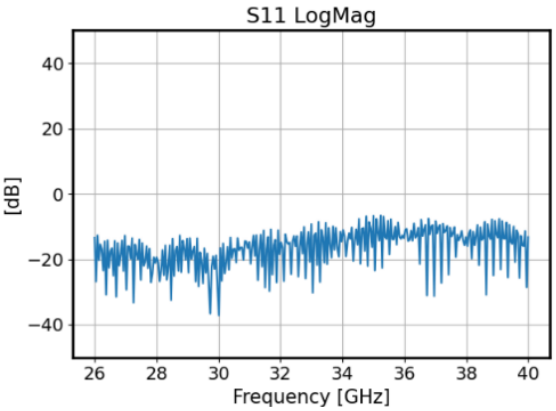

Fig. 12. Measured S-parameter (magnitude of S_{11}) without sample

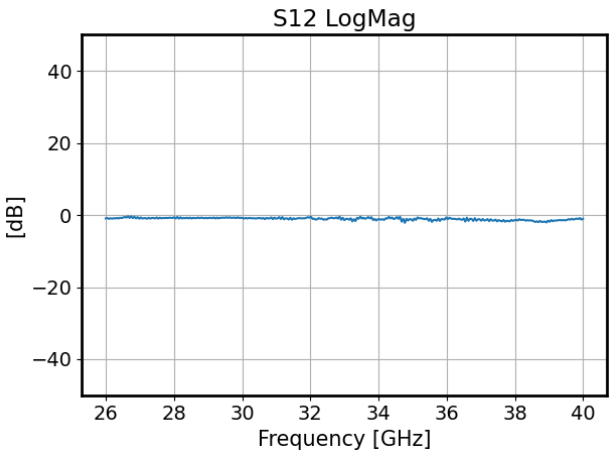

Fig. 13. Measured S-parameter (magnitude of S_{12}) without sample

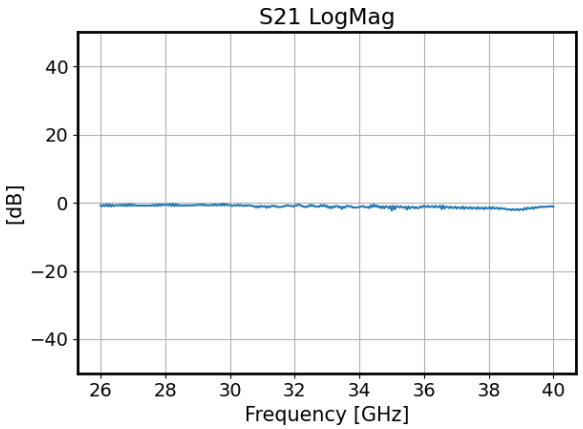

Fig. 14. Measured S-parameter (magnitude of S_{21}) without sample

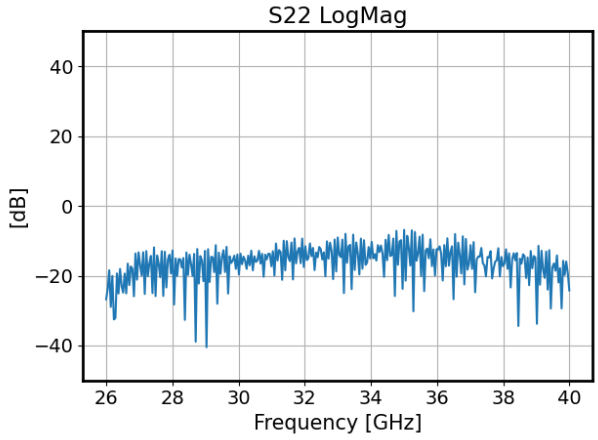

Fig. 15. Measured S-parameter (magnitude of S_{22}) without sample

Meanwhile, Fig. 16–19 show the measured S-parameter (phase) without samples within the 26–40 GHz frequency range. The transmission phases (S_{21} and S_{12}) exhibit a linear and periodic decline with frequency, aligning with the propagation properties of a fixture structure, signifying that the signal undergoes a frequency-dependent phase shift during its passage through the fixture. Conversely, the reflection phases (S_{11} and S_{22}) demonstrate considerable variability with some oscillations, indicating impedance mismatch, numerous reflections, and potential resonant effects at fixture interfaces. The comparatively consistent patterns of S_{21} and S_{12}, in contrast to the irregular S_{11} and S_{22}, indicate that transmission measurements are more dependable for deriving propagation constants and dielectric characteristics, whereas reflection data necessitate further calibration or de-embedding to reduce measurement distortions.

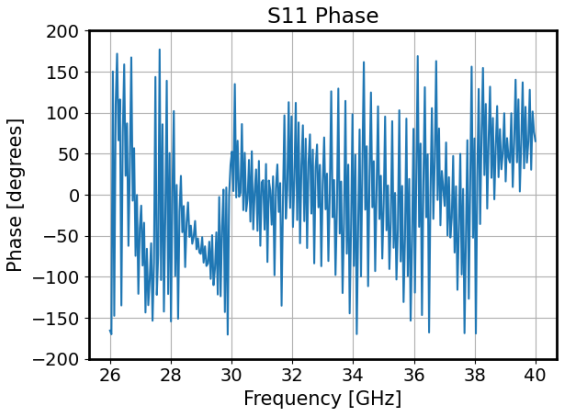

Fig. 16. Measured S-parameter (phase of S_{11}) without sample

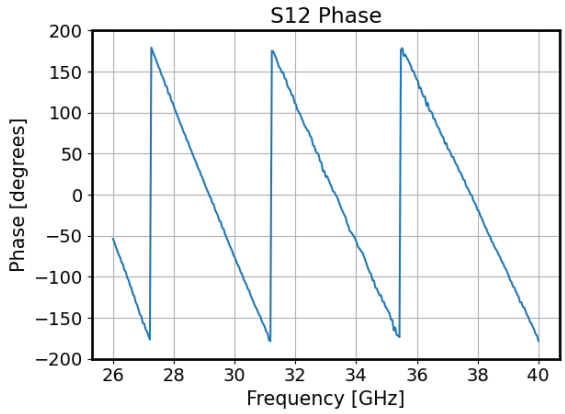

Fig. 17. Measured S-parameter (phase of S_{12}) without sample

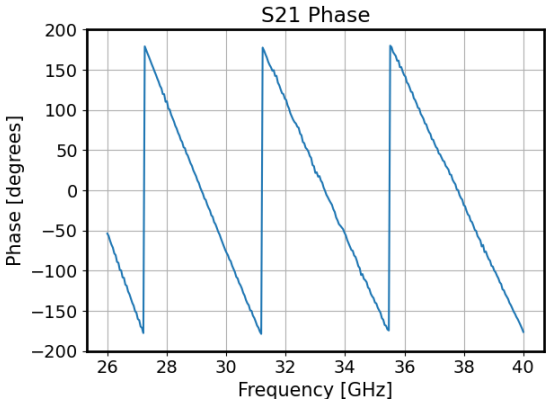

Fig. 18. Measured S-parameter (phase of S_{21}) without sample

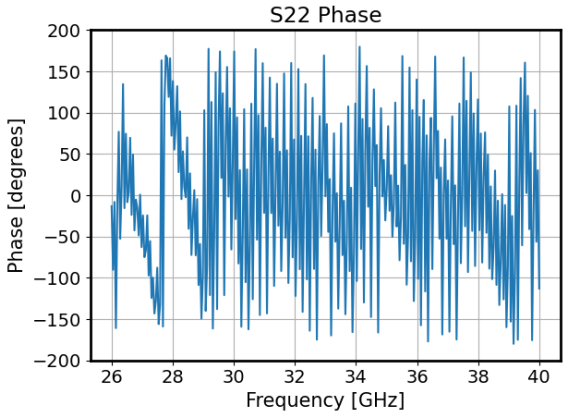

Fig. 19. Measured S-parameter (phase of S_{22}) without sample

Fig. 20(a) shows the extracted permittivity and dissipation factor of one slab of fresh mango leaves. The measured complex permittivity of mango leaves (*Mangifera indica*) over the Ka-band frequency 26–40 GHz reveals a decreasing trend in the real part (ε′). With a maximum of 11.15 at 26 GHz and a minimum of 4.89 at 40 GHz. This decrease supposes a frequency-dependent dielectric dispersion, which is typically explained by polarization mechanisms losing their effectiveness at higher frequencies, especially dipolar and interfacial polarization in the water content and cellular structure of the leaf. The high moisture content of fresh tropical leaves, where bound water relaxation significantly affects permittivity at millimeter-wave frequencies, is consistent with this behavior. These smoothly decreasing permittivity values is similar to those that have been presented on tomato and tobacco dielectric properties extraction [15] and also alfalfa leaves [34].

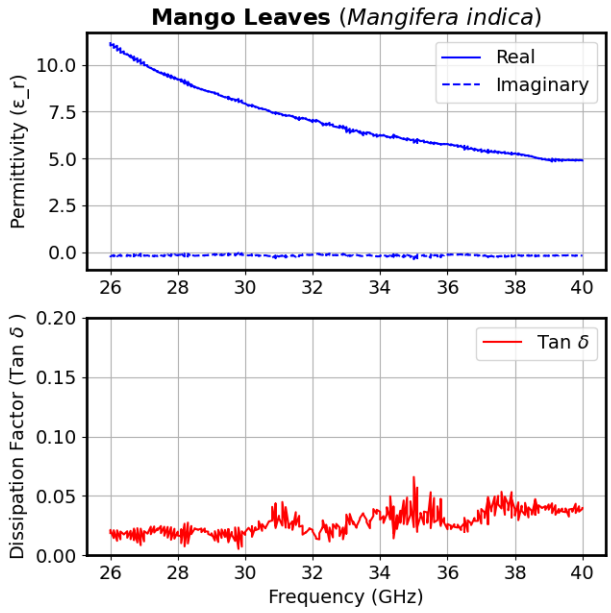

Fig. 20. Complex relative permittivity of SUT (a), dissipation factor (b)

There is little frequency-dependent energy dissipation in the tested band, as indicated by the imaginary part (ε″), which represents dielectric loss remaining comparatively low and stable throughout the frequency range. Together with the real permittivity's observed dispersion, this low loss behavior indicates that, although mango leaves have a sizable dielectric

storage capacity at lower Ka-band frequencies, their absorptive losses are still quite low. This feature is crucial for comprehending foliage-induced attenuation in tropical settings because it suggests that phase delay and scattering, rather than excessive absorption, are the main causes of signal degradation in this range.

Meanwhile, Fig. 20(b) depicted dissipation factor (tan δ) over the tested band. The dissipation factor (tan δ) of mango leaves (*Mangifera indica*) within the frequency range of 26–40 GHz remains consistently low, generally below 0.05, with a maximum value of 0.07, particularly within the 35–38 GHz range, and a minimum value of 0.005. This indicates a small dielectric loss within the spectral range investigated. This indicates that energy dissipation is increased in certain regions, possibly due to resonant interactions between the electromagnetic field and the moisture cell architecture within the leaf.

The very steady and low dissipation factor indicates that attenuation from mango leaves at these frequencies is primarily influenced by scattering and phase delay effects rather than dielectric absorption. This attribute is crucial for millimeter-wave propagation research in tropical settings, indicating that mango leaves, despite exhibiting high real permittivity at lower frequencies within the Ka-band, do not significantly contribute to power loss via absorption. Thus, these findings are important in enhancing foliage attenuation models for 5G and 6G communication systems, especially in rural and semi-urban areas characterized by dense tropical vegetation.

In addition to permittivity and dissipation loss calculation, electrical conductivity (σ) is a key property for describing how materials interact with waves because it measures how well a material can carry an electric current when it comes into contact with an electromagnetic field. Moisture level and ionic concentration in plant tissues have a big effect on conductivity, which affects signal attenuation through ohmic losses. More conductivity means more energy is absorbed and turned into heat, which weakens the signal. This tendency is especially true at higher frequencies, where electrical losses are more noticeable. For this reason, adding conductivity to models of leaf attenuation is necessary to gain a favorable idea of how electromagnetic waves will travel through tropical plants.

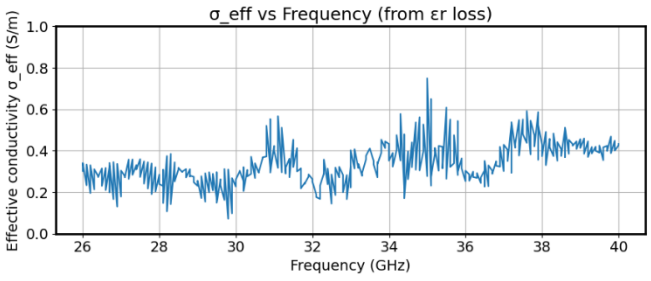

Fig. 21. Calculated conductivity material

Fig. 21 shows the calculated conductivity over the targeted band. The effective conductivity (σ_{eff}) of mango leaves (*Mangifera indica*) in the 26–40 GHz frequency range is from around 0.2 S/m to 0.6 S/m, with considerable variations and occasional peaks above 0.7 S/m at 34–35 GHz. The prevailing trend demonstrates a modest increase in conductivity with frequency, attributable to the augmented contribution of ionic and free water to conduction at elevated millimeter-wave frequencies. The conductivity values, along with permittivity and dissipation factor data, are essential for precise foliage attenuation models, facilitating improved predictions of signal deterioration for Ka-band communication systems in tropical conditions.

This section discusses the influence of sample material thickness on its permittivity value. Accurate measurement of sample thickness is an important factor in determining the permittivity extraction value of a sample. This becomes increasingly urgent if the sample being tested (SUT) is quite thin, as in this study, which involves samples from tropical leaves. Because it's not easy to accurately measure the thickness of thin samples. In this study, it has been shown that after several measurements of sample thickness (t), the average value obtained and its uncertainty are 0.432±0.029 mm, which means that the maximum sample thickness is 0.461 mm and the minimum sample thickness is 0.403 mm. The following section is an analysis of the effect of sample thickness on the extraction permittivity value of the SUT. Fig. 21 shows the effect of thickness variation of the permittivity extraction result.

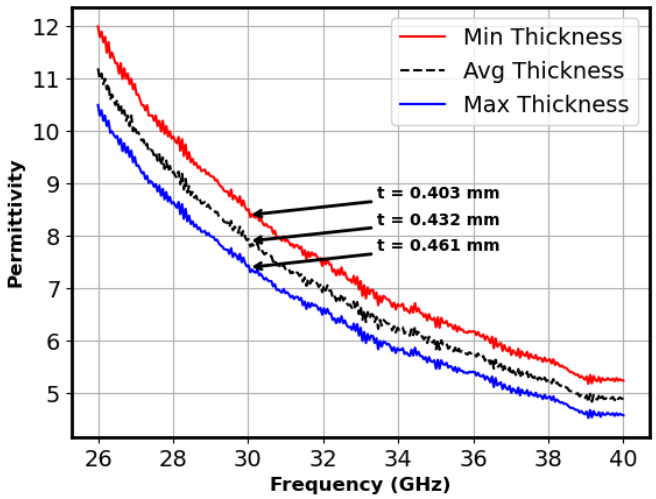

Fig. 22. Thickness variation effect on permittivity extraction result

Fig. 22 illustrates the variation of permittivity (ε_r) of a sample under test across the frequency range of 26–40 GHz for three different thicknesses (minimum, average, and maximum) measurements. In all cases, permittivity decreases monotonically with increasing frequency, indicating typical dielectric dispersion behavior. The highest permittivity values are observed for the minimum thickness sample, reaching 12 at 26 GHz, while the maximum thickness sample exhibits lower values, around 10.5 at the same frequency. As the frequency approaches 40 GHz, the permittivity converges toward values between 4.58 and 5.24, with reduced differences across thicknesses. This trend suggests that thickness variations influence the magnitude of permittivity at lower frequencies but have less effect at higher frequencies, where dielectric response becomes more stable. Overall, the results demonstrate both frequency-dependent dielectric dispersion and sensitivity of permittivity to sample thickness in the Ka-band region.

Several studies have been conducted to identify the permittivity value of materials using various measurement and analysis methods. However, there are only a few studies that focus on finding the permittivity values for natural materials, especially plant leaves. Some of these studies aim to measure the electrical properties of economically important plant leaves, such as tomatoes and corn. It is quite difficult to obtain a truly

comparable study with this research in terms of frequency or the samples used. Nevertheless, Table 3 explains several reports related to this study on premittivity extraction of several leaves at various frequencies.

Table 3. Several previous works on this study

	Material	Frequency	Permittivity
Chauhan et al. [15]	Tomato leaves	100 Hz-1 MHz	1E5-1E4 (highest MC)
	Tobacco leaves	100 Hz-1 MHz	1E7-1E4 (highest MC)
	Tomato leaves	0 – 15 GHz	45-20 (highest MC)
	Tobacco leaves	0 – 15 GHz	50-22 (highest MC)
Shrestha et al. [34]	Alfalfa Leaves	0-20 GHz	42-20 (highest MC)
This Study	Mango leaves	26-40 GHz	16.9-10.8 [13.9 at 28 GHz] (~53% MC)

* MC: Moisture Content

4. Conclusion

The material properties of fresh mango leaves (*Mangifera indica*) measured in the Ka-band frequency range of 26–40 GHz reveal a significant decrease in the real part of permittivity (ε′) with increasing frequency, declining from approximately 11.0 at 26 GHz to around 5.0 at 40 GHz, which indicates noticeable dielectric dispersion resulting from diminished polarization efficiency at high frequencies. The imaginary component (ε″) remains low and rather consistent over the frequency, indicating negligible frequency-dependent absorption losses. The dissipation factor (tan δ) remains constantly below 0.05, with slight peaks, indicating that dielectric storage prevails over absorption in this frequency range. Effective conductivity (σ_{eff}) ranges from 0.2 to 0.6 S/m, with a marginal increase at higher frequencies, indicative of the effects of ionic conduction and moisture content in the leaves. The results suggest that at Ka-band frequencies, signal attenuation through mango foliage is predominantly affected by dielectric dispersion and scattering, rather than significant absorption, highlighting the importance of these parameters for enhancing foliage attenuation models in the planning of tropical millimeter-wave communication systems.

Acknowledgements

This work was conducted as a part of Universiti Teknologi Malaysia (UTM) and Badan Riset dan Inovasi Nasional (BRIN) collaborative research grant vot R.J13000.7351.4B734. This work was partly supported by the BRIN Rumah Program Kegiatan OREI Tahun 2025 Purwarupa Sistem Detektor Bawah Air. The work is also the collaboration between the Lightwave Communication Research Group, Faculty of Electrical Engineering, UTM, and the Radio Frequency Microwave Acoustic and Photonic Communication Research Group, Research Center for Telecommunication, Research Organization for Electronics and Informatics, BRIN.

References

1. A. L. Imoize, O, Adedeji, N. Tandiya, and S. Shetty, *6G Enabled Smart Infrastructure for Sustainable Society: Opportunities, Challenges, and Research Roadmap*. Sensors, 21 (2021) 1709-1767.
2. A. Yazar, S. D. Tusha, and H. Arslan, *6G Vision: An Ultra-Flexible Perspective.* ITU J. Future. and Evolving Technologies, 1 (2020).
3. M, Alsabah, M. A. Naser, B. M. Mahmmoed, S. H. Abdulhussain, M. R. Eissa, and A. Al-Baidani, *6G Wireless Communications Networks: A Comprehensive Survey.* IEEE Access. 9 (2021) 148191-148243.
4. S.T. Rappaport, et al., *Wireless Communications and Applications Above 100 GHz: Opportunities and Challenges for 6G and Beyond.* IEEE Access. 7 (2019) 78729-78757.
5. 5GMF, *5GMF White Paper: 5G Enhancement with millimeter wave deployment*, 3, Editor. (2024).
6. A.G. Siles, Riera M.J., and P. Garcia-Del-Pino, *Atmospheric Attenuation in Wireless Communication Systems at Millimeter and THz Frequencies [Wireless Corner].* IEEE Antennas and Propag. Mag. 57 (2015) 48-61.
7. S. Salous, et al., *Millimeter-Wave Propagation: Characterization and modeling toward fifth-generation systems. [Wireless Corner].* IEEE Antennas and Propag. Mag. 58 (2016) 115-127.
8. C. Zang, Z, Ma, J, Wang, Y, Yao, X, Han, and X, He, *Measurement, data analysis and modeling of electromagnetic wave propagation gain in a typical vegetation environment.* PLOS ONE. 18 (2023) 1-24.
9. J. Isabona, A. L. Imoize, S. Ojo, C. C. Lee, and C. T. Li. *Atmospheric Propagation Modelling for Terrestrial Radio Frequency Communication Links in a Tropical Wet and Dry Savanna Climate*. Information, 13 (2022).
10. J. A. Azevedo, and F. E. Santos, *A model to estimate the path loss in areas with foliage of trees.* AEU - Int. J. Electron. Commun, 71 (2017) 157-161.
11. F.T. Ulaby, , R.K. Moore, and A.K. Fung, *Microwave remote sensing: active and passive, Vol. III: From Theory to Application*. (1986): Artech House, Inc.
12. N. Chitraningrum, et al., *Microwave absorption properties of porous activated carbon-based palm oil empty fruit bunch.* AIP Adv., 12 (2022).
13. N. Chitraningrum, et al., *Preparation and characterization of porous carbon-based oil palm empty fruit bunch as a candidate material for an electromagnetic waves absorber application.* AIP Conf. Proc, 2024. 2973 (2024) 060012.
14. H. Ma'rufah, H.L. Nugroho, and S. Sukirno, *Effectiveness extract of Crataeva nurvala leaves as insecticide against Spodoptera litura.* Commun. Sci. Technol, 9 (2024) 310-321.
15. D.P. Chauhan, H.D. Gadani, and A.V. Rana, *Dielectric properties of tobacco and tomato plant leaves over a broad frequency range.* J. Microwave Power Electromagn. Energy, 57 (2023) 278-289.
16. B. Itolikar, A. and M.L. Kurtadikar, *Microwave Dielectric Properties and Emissivity Estimation of Freshly Cut Banana Leaves at 5 GHz.* Int. J. Adv Remote Sensing and GIS, 5 (2017).
17. M.S. Venkatesh and G.S.V. Raghavan, *An overview of dielectric properties measuring techniques.* Can. Biosyst. Eng., (2005).
18. T. Mosavirik, M.S., V. Nayyeri, S. H. Mirjahanmardi and O. M. Ramahi, *Permittivity Characterization of Dispersive Materials Using Power Measurements.* IEEE Trans. Instrum. Meas, 70 (2021).
19. N. Billings, A. Birjiniuk, T. S. Samad, P. S. Doyle, and K. Ribbeck, *Material properties of biofilms—a review of methods for understanding permeability and mechanics.* Rep. Prog. Phys, 2015. 78 (2015) 036601.
20. F. M. Al-Oqla, S. M. Sapuan, T. Anwer, M. Jawaid, and M. E. Hoque, *Natural fiber reinforced conductive polymer composites as functional materials: A review.* Synth. Met., 206 (2015) 42-54.

21. R. Testa, S. Tudisca, G. Schifani, A. M. D. Trapani, and G. Migliore, *Tropical Fruits as an Opportunity for Sustainable Development in Rural Areas: The Case of Mango in Small-Sized Sicilian Farms*. Sustainability, 10 (2018).
22. S.F.P. Júnior, et al., *Characterization of the Dielectric Properties of the Tommy Atkins Mango.* J. Microwaves, Optoelectronics and Electromag. App., 19 (2020) 86-93.
23. S, Wang, M. Monzon, Y. Gazit, J. Tang, E. J. Mitcham, and J. W. Armstrong, *Temperature-Dependent Dielectric Properties of Selected Subtropical And Tropical Fruits And Associated Insect Pests.* Trans. Am. Soc. Agric. Eng, 48 (2025) 1873-1881.
24. V. C. Vanderbilt, and L. Grant, *Plant Canopy Specular Reflectance Model.* IEEE Trans. Geosci. Remote Sens., GE-23 (1985) 722-730.
25. S. A. R. Khatik and D. V. Ahire, *Correlations of Complex Dielectric Constant of Tree Leaves with Their Chemical Properties at X-Band Frequency.* Int. J. Innovative Research Sci., Eng. Tech., 6 (2017) 7-13.
26. S. Metlek, K. Kayaalp, I. B. Basyigit, A. Genc, and H. Dogan, *The dielectric properties prediction of the vegetation depending on the moisture content using the deep neural network model.* I. J. RF Microwave Comput. Aided Eng., 31 (2021).
27. P. Chauhan, D. H. Gadani, and V.A. Rana, *Study of variation of complex permittivity of tree leaves with moisture content, over microwave frequency range.* Mater. Today: Proc.., 67 (2022).
28. W. B. Weir, *Automatic Measurement of Complex Dielectric Constant and Permeability at Microwave Frequencies.* Proc. IEEE, 62 (1974) 33-36.
29. Y. Ye, A. Sklyuyev, C. Akyel, and P. Ciureanu. *Automatic System to Measure Complex Permittivity and Permeability using Cavity Perturbation Techniques*. in *Instrumentation and Measurement Technology Conference-IMTC 2007*. (2007).
30. A. M. Nicolson, and G.F. Ross, *Measurement of the Intrinsic Properties of Materials by Time-Domain Techniques*, in IEEE Trans. Instrum. Meas. (1970).
31. A. L. D. Paula, M. C. Rezende, and J. J. Barroso. *Modified Nicolson-Ross-Weir (NRW) method to retrieve the constitutive parameters of low-loss materials*. in *2011 SBMO/IEEE MTT-S Int. Microwave Optoelectron Conf.*. 2011. IEEE. (2011).
32. D. R. Smith, S. Schultz, P. Markos, C. M. Soukoulis , *Determination of effective permittivity and permeability of metamaterials from reflection and transmission coefficients.* Phys. Rev. B, 65 (2002).
33. L. F. Chen, C. K. Ong., C. P. Neo, V. V. Varadan, and V. K. Varadan, *Microwave Electronics: Measurement and Materials Characterization*. 2004: John Wiley & Sons Ltd.
34. B. L. Shrestha, H. C. Wood and S. Sokhansanj. *Microwave Dielectric Properties of Alfalfa Leaves From 0.3 to 18 GHz.* IEEE Trans. Instrum. Meas., 60 (2011).